



HHS Public Access

Author manuscript

J Biomol Screen. Author manuscript; available in PMC 2016 July 01.

Published in final edited form as:

J Biomol Screen. 2015 July ; 20(6): 801–809. doi:10.1177/1087057115575150.

A High-Throughput Enzyme-Coupled Assay for SAMHD1 dNTPase

Kyle J. Seamon¹ and James T. Stivers¹

¹Department of Pharmacology and Molecular Sciences, The Johns Hopkins University School of Medicine, Baltimore, MD, USA

Abstract

Sterile alpha motif and histidine-aspartate domain-containing protein 1 (SAMHD1) is a recently discovered enzyme that plays a central role in nucleotide metabolism and innate immunity. SAMHD1 has deoxyribonucleoside triphosphate (dNTP) triphosphohydrolase activity that depletes the dNTP substrates required for DNA synthesis in cells. The involvement of SAMHD1 in biological processes as varied as viral restriction, endogenous retroelement control, cancer, and modulation of anticancer/antiviral nucleoside drug efficacy makes it a valuable target for the development of small-molecule inhibitors. We report a high-throughput colorimetric assay for SAMHD1 dNTP hydrolase activity that takes advantage of *Escherichia coli* inorganic pyrophosphatase to convert PPP_i to $3 P_i$. The assay was validated by screening a library of 2653 clinically used compounds. Fifteen primary hits were obtained (0.57% hit rate); 80% of these were confirmed in a direct secondary assay for dNTP hydrolysis. The zinc salt of the antibiotic cephalosporin C was a potent inhibitor of SAMHD1 with an IC_{50} of $1.1 \pm 0.1 \mu M$, and this inhibition was largely attributable to the presence of zinc. The assay also screened a targeted library of nucleosides and their analogs, revealing that the antiviral drug acycloguanosine (acyclovir) is an inhibitor possessing excellent properties for future fragment-based drug development efforts.

Keywords

innate immunity; viral restriction; nucleotide metabolism; high-throughput screening

Introduction

Sterile alpha motif and histidine-aspartate domain-containing protein 1 (SAMHD1) is tetrameric deoxyribonucleoside triphosphate (dNTP) triphosphohydrolase that disrupts the synthesis of nonhost nucleic acids. SAMHD1 is composed of two domains: an N-terminal

© 2015 Society for Laboratory

Corresponding Author: James T. Stivers, Department of Pharmacology and Molecular Sciences, The Johns Hopkins University School of Medicine, 725 North Wolfe Street, Baltimore, MD 21205-2185, USA., jstivers@jhmi.edu.

Declaration of Conflicting Interests

The authors declared no potential conflicts of interest with respect to the research, authorship, and/or publication of this article.

Supplementary material for this article is available on the *Journal of Biomolecular Screening* Web site at <http://jbx.sagepub.com/supplemental>.

sterile alpha motif (SAM) domain of unknown function and a C-terminal histidine-aspartate (HD) domain with metal-dependent phosphohydrolase activities. Upon activation by dGTP or GTP, the activity of the HD domain catalyzes the hydrolysis of any dNTP to its deoxyribonucleoside (dN) and triphosphate (PPP_i).¹ Crystal structures and biochemical analyses have shown that activation by binding of guanine nucleotides to a guanine-specific activator (A1) precedes the binding of dNTPs to a second nonspecific activator (A2) site on each monomer, which in turn drives the formation of the catalytically competent tetramer.²⁻⁴ SAMHD1 also has activator-independent RNA binding and exonuclease activities,^{5,6} although the presence of the nuclease activity has been disputed.¹

SAMHD1 is found across many cell types⁷ but is most highly expressed in immune cells of the myeloid lineage, where it acts as a viral restriction factor.⁸ The SAMHD1-catalyzed depletion of dNTP pools in these cells restricts infection of diverse retroviruses⁹ and DNA viruses¹⁰ by depriving the viral DNA polymerases of dNTP building blocks. SAMHD1-mediated restriction of HIV-1 infection in dendritic cells prevents the activation of CD4+ T cells and, paradoxically, dampens subsequent adaptive immune responses.¹¹ Although SAMHD1 inhibits the productive infection of myeloid immune cells, the aborted reverse transcripts that accumulate in these cells triggers an inflammatory response and death of bystander CD4+ T cells in a process termed *pyroptosis*.¹² Inhibition of SAMHD1 would prevent the accumulation of aborted transcripts and would therefore be expected to prevent T-cell depletion in response to HIV infection and possibly slow the progression to AIDS.

SAMHD1 also has essential roles in nucleotide metabolism and homeostasis.^{7,13} Loss-of-function mutations in SAMHD1 are associated with autoimmune disorders such as the inheritable neuroinflammatory disease Aicardi-Goutières syndrome (AGS)¹³ and the inflammatory disease systemic lupus erythematosus (SLE).¹⁴ Both AGS and SLE stem from an immune response to aberrant intracellular nucleic acids that mimic chronic viral infection.¹⁵ Loss-of-function mutations in SAMHD1¹⁶ or epigenetic silencing of the SAMHD1 locus¹⁷ are also associated with the development of various cancers, possibly through increased mutation rates caused by dNTP pool imbalances.¹⁸ SAMHD1 expression also increases the efficacy of nucleoside drugs that are used to treat viral infections and cancer, likely by decreasing the concentration of competing intracellular dNTPs.¹⁹

The involvement of SAMHD1 in the above biological processes motivates inhibitor design for both basic science and potential clinical applications. The large number of nucleotide binding sites (12 per tetramer) and the need for allosteric activation and oligomerization suggest that SAMHD1 would be highly amenable to inhibition by small molecules. Indeed, we have designed a nucleotide analog that inhibits SAMHD1 by the surprising mechanism of destabilizing the catalytically competent tetramer,²⁰ but the utility of this compound was limited by poor bioavailability. Here we report a cost-effective high-throughput colorimetric screen for SAMHD1 dNTPase activity using *Escherichia coli* inorganic pyrophosphatase as a coupling enzyme for the detection of inorganic phosphate. This method can be readily applied to screen large chemical libraries for inhibitors of SAMHD1 that could be functional in cell culture. Such inhibitors would be especially valuable for investigating the function of SAMHD1 in primary immune cells that are genetically difficult to manipulate. Specific inhibitors of the dNTPase activity would be particularly useful to determine whether the

dNTPase or the RNA exonuclease activity of SAMHD1 is responsible for retroviral restriction and retroelement control as these roles are currently disputed in the literature.^{6,8}

Materials and Methods

Human SAMHD1 Overexpression and Purification

Full-length human SAMHD1 was expressed as a PreScission protease-cleavable His₁₀ fusion in *E. coli* BL21-DE3 cells and purified by Ni-NTA and cation exchange chromatography as described previously.⁴ The protein concentration was calculated by its absorbance at 280 nm using an extinction coefficient of 76,500 M⁻¹ cm⁻¹ (ProtParam, ExPASy). Typical yields were 20 mg of SAMHD1 per liter of bacterial growth with an estimated purity of >95% as determined from sodium dodecyl sulfate–polyacrylamide gel electrophoresis (SDS-PAGE) with visualization by Coomassie blue staining. The purified protein (100 μM) was flash frozen in small aliquots (20 to 50 μL) at –80 °C in storage buffer (50 mM Tris-HCl [pH 7.5], 150 mM KCl, 5 mM MgCl₂, 1 mM DTT, 20% glycerol). Thawed aliquots for activity assays were stored at –20 °C for a maximum of 3 d before discarding.

Inorganic Pyrophosphatase (PPase) Overexpression and Purification

The inorganic pyrophosphatase gene with its native promoter, Shine-Dalgarno sequence, and terminator was PCR-amplified from *E. coli* K12 genomic DNA using oligonucleotide primers (forward: 5' ATT TTA GGA TCC AGA CGA AAA CAA GCG AAG ACA TTC 3'; reverse: 5' ATT TTA AAG CTT GTG TGT TTA TTT ATC GCG GGC). The PCR product was ligated into the BamHI and HindIII sites of pUC19, and the sequence of the insert was verified by sequencing. The plasmid (pUC19-PPase) is available upon request. *E. coli* DH5α cells were transformed with pUC19-PPase and grown in LB medium at 37 °C for 15 h. The cells were harvested by centrifugation, and the cell pellets were stored at –80 °C until purification. The cell pellet was resuspended in lysis buffer (50 mM Tris-HCl [pH 7.5], 100 mM NaCl, 1 mM EDTA, 0.1% Triton X-100, protease inhibitors [Sigma P2714], and 0.5 mg/mL lysozyme) and rotated at 4 °C for 1 h. The crude lysate was clarified by centrifugation at 30,000 g for 30 min at 4 °C. Nucleic acid was precipitated by the slow dropwise addition of one-half volume of cold 10% streptomycin sulfate on ice. The nucleic acid was removed by centrifugation at 30,000 g for 30 min at 4 °C. The supernatant was adjusted to 20 mM MgCl₂ by addition of 2 M MgCl₂ stock, then heated in a 70 °C water bath for 30 min. The solution was returned to ice for 30 min, and the precipitated protein was removed by centrifugation at 30,000 g for 15 min at 4 °C. The supernatant (which contains PPase) was warmed to 20 °C and adjusted to 70% saturated ammonium sulfate. The solution was stirred for 30 min, and the protein precipitate (containing PPase) was collected by centrifugation at 30,000 g for 30 min at 20 °C. The pellet was resuspended in a minimal volume of storage buffer (50 mM Tris-HCl [pH 8.0], 150 mM NaCl, 5 mM MgCl₂, 1 mM DTT, 30% glycerol) and dialyzed overnight at 4 °C. The purified protein (900 μM) was aliquoted (500 μL) and stored at –20 °C. The PPase concentration was determined using the Bradford assay with bovine serum albumin as the standard. Typical yields were 200 mg/L pyrophosphatase with >75% purity by SDS-PAGE, which is sufficient for the

screening assay. We found that the activity of PPase obtained from this method was identical to commercially available preparations (Sigma I5907).

Enhanced Malachite Green (MG) Assay for SAMHD1 dNTPase Activity

Because SAMHD1 produces PPP_i and a dN as products, the PPP_i product was converted to inorganic phosphate (P_i) in a coupled reaction with pyrophosphatase before detection colorimetrically using the well-known MG phosphate detection reagent.²¹ A working stock of MG solution was prepared by dissolving 0.40 g of MG hydrochloride (Sigma M9636) in a 360 mL solution consisting of 300 mL ddH₂O and 60 mL concentrated H₂SO₄ (JT Baker 9681). Separate ddH₂O stocks of 7.5% (w/v) ammonium molybdate tetrahydrate (Fluka 09880) and 11% (v/v) Tween-20 (Sigma P7949) were prepared. The MG detection reagent was prepared fresh daily by mixing 20 mL of the MG solution with 5 mL of ammonium molybdate and 0.4 mL of Tween-20 solution. Standard curves for phosphate detection were prepared in clear polystyrene round-bottom 96-well plates (Costar 3795) by serial dilution of a standard solution (80 μ L final well volume; Ricca Chemical Company 5839). Flat-bottom 96-well plates performed similarly and can be substituted if desired. The phosphate standards used the same buffer and quench conditions as the enzymatic reactions (see below). The MG detection reagent was added in a ratio of 1:4 (20 μ L of detection reagent to 80 μ L of reaction solution). Plates were mixed by rotary shaking at 780 rpm for 30 s and were then incubated at room temperature for 90 to 240 min. The increased incubation time in this enhanced version of the MG assay increases the linear range for P_i detection and the overall signal-to-background of the assay (see the Results section). The absorbance at 650 nm for each well was measured by Multiskan Ascent plate reader (Labsystems).

In the high-throughput screening (HTS) format, SAMHD1 reactions were performed in a total volume of 40 μ L (50 mM Tris-HCl [pH 7.5], 50 mM KCl, 5 mM MgCl₂, 0.05% Brij-30) using 96-well round-bottom plates. All liquid dispensing was performed using a TomTec Quadra 96–320 liquid handler with reagents aspirated from polypropylene storage plates (Costar 3363) or deep-well assay blocks (Costar 3959). Positive control reactions (no inhibitors) were prepared by aspiration of 10 μ L of a mock solution consisting of buffer and 4% DMSO, 20 μ L of substrate solution consisting of 0.2 mM dGTP in 2 \times reaction buffer, and 10 μ L enzyme solution consisting of 2 μ M SAMHD1 and 20 μ M PPase into a single tip with 20 μ L air gaps separating each solution. The reagents were dispensed into wells with a 20 μ L air blowout and touch off, and the plates were immediately mixed by rotary shaking. The final concentrations of all components in each reaction well are listed in Table 1. Controls established that the final concentration of 1% DMSO has no effect on the SAMHD1 activity. Reaction quench solutions were prepared by aspiration of 40 μ L of 20 mM EDTA and 20 μ L of MG detection solution into each tip using a 20 μ L air gap separation and then dispensing the quench solutions into the reaction wells using a 20 μ L air blowout and touch off. After quenching, the plates were mixed by rotary shaking and the absorbance was measured as above after a 90 min incubation. The phosphate present in each well was determined by comparison with a standard phosphate curve.

Pilot Library Screening

The optimized SAMHD1 assay was used to screen a pilot library of 2653 clinically used compounds (a generous gift of Dr. Jun O. Liu). The reactions were performed in reaction buffer with final concentrations of 0.5 μ M SAMHD1, 5 μ M PPase, 0.1 mM dGTP, 1% DMSO, and 10 μ M library compound prepared as described above. After 20 min, reactions were quenched with EDTA and the MG detection reagent, and the absorbance was measured after 90 min color development time as described above. Each screening plate contained 80 compounds and 16 DMSO-only controls. Half of the DMSO-only control wells were used for the SAMHD1 + PPase positive activity controls and the remaining were used for the PPase-only negative activity controls. The percentage SAMHD1 activity that remained in each compound well was calculated from the average of the positive and negative control reactions on that plate (% activity remaining = $100 \times (A_{\text{well}} - \langle A_{\text{neg}} \rangle) / (\langle A_{\text{pos}} \rangle - \langle A_{\text{neg}} \rangle)$), where A_{well} is the absorbance of a well containing a library compound and $\langle A_{\text{pos}} \rangle$ and $\langle A_{\text{neg}} \rangle$ are average absorbance values for the control wells for the same plate. The Z' statistical factors for each plate were calculated using eq 1.²²

$$Z' = 1 - \frac{3(SD_{\text{pos}} + SD_{\text{neg}})}{\langle A_{\text{pos}} \rangle - \langle A_{\text{neg}} \rangle} \quad (1)$$

Thin-Layer Chromatography (TLC) Secondary Assay

Compounds that were identified as hits in the primary enzyme-coupled MG assay were confirmed using a direct TLC assay that separates the dNTP substrate from the nucleoside product.⁴ In the secondary assay, SAMHD1 reactions were prepared under the same conditions as in the MG assay, except that PPase was omitted and the dGTP substrate was spiked with trace amounts of tritium-labeled [8-³H]dGTP. Small portions (2 μ L) were quenched at various times by direct spotting on a C18 reversed-phase TLC plate. The TLC plates were developed and quantified as described previously to obtain a reaction rate for each inhibitor, which was compared with a DMSO control.⁴

Dose-Response Curves and IC₅₀ Determinations

Dose-response curves were performed using the MG assay. Master solutions of each compound were prepared from the solids and were serially diluted by twofold into enzyme reactions. The reactions were otherwise carried out exactly as described above. The percentage SAMHD1 activity remaining as a function of inhibitor concentration was fit to eq 2 employing a variable Hill slope parameter

$$\% \text{Activity Remaining} = \min + \frac{(\max - \min)}{1 + 10^{h(\log \text{IC}_{50} - \log[\text{Inhibitor}])}} \quad (2)$$

where max and min are the maximal and minimal percentage activity values and h is the Hill slope using the program Prism 6 (GraphPad Software).

Results and Discussion

Enzyme-Coupled MG Assay

The triphosphohydrolase reaction catalyzed by SAMHD1 produces dN and triphosphate products, neither of which is directly amenable to high-throughput detection. However, reliable colorimetric²¹ and fluorescent²³ methods do exist for the detection of free inorganic phosphate (P_i). We therefore envisioned an assay in which the production of triphosphate by SAMHD1 was coupled to the detection of P_i by enzymatic PPP_i hydrolysis. To be feasible in this application, the coupling enzyme should be easy to purify in high yields and highly specific for the desired PPP_i product with little or no activity on the dNTP substrate. We found that inorganic pyrophosphatase (PPase) from *E. coli* satisfies these requirements. We thus optimized a chromatography-free purification procedure that gives a high yield (200 mg/L) of active PPase of sufficient purity for screening and determined that it has minimal activity on the dGTP substrate of the SAMHD1 reaction (see below).

Optimization of the MG Assay

A simple and economical method for detecting P_i is the change in absorbance of a solution of MG and molybdate upon complexation with phosphate.²¹ Although a continuous enzyme-coupled assay for P_i exists,²³ this assay is prohibitive to implement in an HTS format because it requires stoichiometric complexation of phosphate binding protein with P_i . In contrast, the MG assay is easy to implement and requires only inexpensive reagents.

MG has been used to detect phosphate in many applications,²¹ but we were initially disappointed in the linear range and signal-to-background obtained using reported methods. Nevertheless, by simply increasing the incubation time for development of the MG complex from 10 to 90 min before making the absorbance measurements, we were able to extend the linear range for phosphate detection from 4 to 12 nmol (Suppl. Fig. S1A). This key improvement allows us measure a greater extent of reaction and take full advantage of the three equivalents of P_i that are produced from each mol of PPP_i product. Thus, the favorable features of our enhanced MG assay include (1) the excellent linearity up to 12 nmol P_i ($r^2 > 0.9985$; Fig. 1A), (2) the color stability from 1.5 to 4 h after addition of the MG detection reagent (Suppl. Fig. S1B), and (3) the increased signal-to-background as compared with a standard MG assay.

Pyrophosphatase Coupling Reaction

For an enzyme-coupled reaction to be useful, the coupling enzyme must be present in sufficient quantity such that its reaction is fast compared with the reaction of interest. To determine the PPase concentration that was required to meet this condition, a series of experiments were performed in which the SAMHD1 and dGTP substrate concentrations were fixed at the desired concentrations for the HTS and the PPase concentration was varied from 1 to 9 μ M. From this analysis, we ascertained that the rate of P_i formation was zero-order in [PPase] when its concentration exceeded about 5 μ M (Suppl. Fig. S1C, D). There was little color development when 5 μ M PPase was incubated with 0.1 mM dGTP in the absence of SAMHD1, indicating that PPase is reacting with the PPP_i product and not the dGTP substrate (Fig. 1B). The observed rate of P_i production was linear to at least 80%

dGTP hydrolysis, indicating that the endpoint of the HTS could be chosen within this broad range. The linearity of product formation over such a large extent of reaction is surprising given that the concentration of the dGTP activator (and substrate) is slightly greater than the apparent K_{act} and 10-fold less than the apparent K_m value reported in our previous biochemical studies with SAMHD1.⁴ In this prior work, we showed that the catalytically competent homotetramer is exceedingly stable once it is formed, remaining active for many hours even after removal of activating nucleotides (i.e., hysteresis). Thus, depletion of the dGTP activator during the short time course of the MG assay would not decrease the activation level of the enzyme. Although 80% depletion of the dGTP substrate would be expected to decrease the reaction rate based on its initial concentration and its apparent K_m value, the complex nature of the ordered-essential activation mechanism and the unusual hysteresis make it difficult to predict when zero-order reaction kinetics would be observed. Furthermore, the pyrophosphatase-coupled degradation of the triphosphate product would also contribute to the extended linear range of the reaction progress curve by preventing product inhibition and increasing the thermodynamic driving force for the dNTPase reaction. None of this complexity affects the reliability or utility of the HTS.

We note that during our HTS optimization, another group reported an MG-based colorimetric assay for SAMHD1 but did not report its use in an HTS application.²⁴ Our enhanced MG assay has several advantages over this previous version. First, the reported assay employed yeast exopolyphosphatase to couple the production of PPP_i to detection of $P_i + PP_i$. Because our assay uses PPase as the coupling enzyme, PPP_i is converted completely to $3P_i$, and the color yield per PPP_i is threefold greater. This also has significant cost benefits because the enhanced assay uses one-tenth the concentration of the dGTP substrate as compared with the reported assay, and dGTP is the major contributor to the assay cost. Second, bacterial expression of recombinant yeast exopolyphosphatase is only 0.5% the level of pyrophosphatase, and its purification involves more steps and expensive resins.²⁵ Third, our enhanced assay uses a 10-fold lower concentration of full-length SAMHD1 enzyme as opposed to the N-terminal truncated form used in the published MG assay. We have found that the N-terminal truncation reduces the maximal activity by about 50% as compared with full-length SAMHD1. In general, it is always more desirable to screen the enzyme form that is expressed in cells.⁴

Development of the HTS

Based on the time dependence of the SAMHD1 reaction under the desired conditions of the HTS, a 20-min reaction time was selected that corresponded to about 75% reaction. To test the statistics and reproducibility of the enhanced MG assay under these conditions, two 96-well plates of replicate reactions containing either SAMHD1 and PPase (positive control) or PPase alone (negative control) were prepared. The two plate sets showed low well-to-well variation (coefficient of variation = 3.3% and 3.4%), and the mean absorbance increase was 2.02 ± 0.08 between the reactions in the presence and absence of SAMHD1, corresponding to a signal-to-background of nine (Fig. 1C, D). The high $Z' = 0.87$ and the low coefficients of variation in both the positive and negative control wells indicate that this assay has favorable properties as an HTS.²² The optimized assay conditions and statistical parameters for the 96-well format are summarized in Table 1. The expected reaction volumes and cost

per well would be halved upon miniaturization to 384-well plates (and even further for a 1536-well format), while the compound throughput would increase approximately fourfold.

Pilot Library Screening

The optimized assay was used to screen a library of 2653 clinical compounds.²⁶ The screening results approximated a normal distribution with a mean around 95% of the activity of the DMSO-only controls (Fig. 2A, B). Setting a hit threshold of 3σ below the mean ($<71.5\%$ activity), 29 hits were obtained (1.1% hit rate). A more stringent cutoff of 6σ ($<48\%$ activity) yielded 15 hits (0.57% hit rate). The Z' factors calculated from the eight positive and negative control wells on each plate gave an excellent average Z' of 0.90 ± 0.04 (Fig. 2C). Although this library is relatively small, it has a representative chemical diversity suggesting that the screen can be readily applied to larger libraries.

Hit Validation

The 6σ cutoff was used to focus on 15 hits that were detected in the primary screen. The secondary screen uses reversed-phase TLC separation of [^3H]-dGTP from the nucleoside product.⁴ This is a rapid and economical secondary screen that can be used to make single-time-point activity determinations on hundreds of compounds in several hours using a 12-channel pipettor. Of the 15 compounds tested, 12 showed similar or greater inhibition in this direct assay, corresponding to a validation rate of 80% (Fig. 3A). The structures of these hits as well as their activity in the MG primary and TLC secondary screen are shown in Supplementary Table S1. The majority of these hits were nuisance compounds with attributes that are known to cause promiscuous inhibition or were otherwise undesirable (catechols, heavy metals, Michael acceptors, etc.). However, two salt forms of the β -lactam antibiotic cephalosporin C (Ceph C) were verified as hits. Ceph C was also of note because of its apparent specificity; 30 other cephalosporins in the library showed no significant inhibition.

The Zn^{2+} salt of Ceph C was obtained as a solid for further analysis. We were unable to procure the sodium salt from any commercial vendor, so it was generated from the Zn^{2+} salt by ion exchange using Dowex- Na^+ resin. Dose-response studies using the two salt forms of Ceph C showed that the Zn^{2+} salt was a 200-fold more potent inhibitor ($\text{IC}_{50}^{\text{CC-Zn}} = 1.1 \pm 0.1 \mu\text{M}$, $h = 1.4 \pm 0.1$; $\text{IC}_{50}^{\text{CC-Na}} = 213 \pm 30 \mu\text{M}$, $h = 0.8 \pm 0.1$; Fig. 3B).

Some cephalosporin antibiotics are known to form tight complexes with divalent metal ions,²⁷ including Zn^{2+} , which suggested that the inhibition might result from an E- Zn^{2+} -Ceph C enzyme-metal-bridged complex. However, further investigation showed that Zn^{2+} alone (as the chloride salt) was also inhibitory ($\text{IC}_{50}^{\text{Zn}} = 2.1 \pm 0.2 \mu\text{M}$, $h = 1.2 \pm 0.1$; Fig. 3B). The inhibition of SAMHD1 by Zn^{2+} ions even in the presence of 5 mM MgCl_2 has not been investigated previously, although crystal structures have been reported that use Zn^{2+} as a catalytically inert metal.² The inhibition by Ceph C- Zn^{2+} and Zn^{2+} alone was completely rescued by the addition of approximately stoichiometric amounts of EDTA, which selectively chelates Zn^{2+} over Mg^{2+} (Suppl. Fig. S2). Although these data indicate that Zn^{2+} alone inhibits SAMHD1, the fact that Ceph C itself is weakly inhibitory, combined with the enhanced inhibition observed with Ceph C- Zn^{2+} , does not exclude the possibility of a E-

Zn²⁺-Ceph C bridge complex. However, given the low levels of free Zn²⁺ in cells,²⁸ it is very unlikely that such a complex would have biological activity. We note that the Zn²⁺ dependence of Ceph C inhibition is evocative of the diketo acid metal chelate inhibitors of HIV integrase.²⁹ These potent inhibitors coordinate divalent cations and are significantly more inhibitory in their metal-complexed form.²⁹ These similarities suggest that metal chelation approaches should be actively explored in inhibitor development against SAMHD1.

Screening of Nucleosides and Nucleoside Analogs

The unique activation mechanism of SAMHD1, which involves binding of activating nucleotides to two proximal binding pockets on the enzyme surface, makes it an excellent target for fragment tethering-based strategies. In this regard, nucleoside fragments have proved to be useful starting fragments for the development of inhibitors of enzymes involved in nucleotide metabolism. One example was our finding that a uracil substrate fragment could serve as a starting scaffold for development of a potent inhibitor of human dUTP hydrolase (dUTPase) by fragment tethering.³⁰ Medicinal chemistry efforts by Taiho Pharmaceuticals have built on the uracil fragment to yield a potent inhibitor of dUTPase that is in clinical trials.

To identify a potential inhibitory nucleoside fragment that targets SAMHD1, dose-response curves were obtained for the canonical dNs: deoxythymidine (dThy), deoxycytosine (dCyt), deoxyuridine (dUrd), deoxyadenosine (dAdo), and deoxyguanosine (dGuo; Fig 4A). Of these, only dGuo showed significant inhibition ($IC_{50} = 488 \pm 50 \mu M$, $h = 1.0 \pm 0.1$), probably because of its binding in the guanine nucleoside-specific A1 activator site.^{2,4} The structural requirements for binding were further explored using several analogs of deoxyguanosine (Fig. 4B, C). Several important structure-activity relationships were obtained from these results: (1) the exocyclic amine of guanine is important for binding because dIno, which lacks this amine, is significantly less inhibitory; (2) the conformation and/or steric features of the ribose ring are important because the rGuo and ddGuo analogs show significantly weaker inhibition; and (3) a sugar ring is not critical for inhibition because acGuo (acycloguanosine or acyclovir) inhibits with potency similar to dGuo itself ($IC_{50} = 764 \pm 82 \mu M$, $h = 1.0 \pm 0.1$).

The identification of acyclovir as an inhibitor is potentially useful for fragment tethering studies because of its small size (MW = 225 g/mol) and the absence of the ribose ring that is prone to ring-opening and anomerization reactions. In addition, this simple nucleoside fragment has a limited number of nucleophilic moieties that would need to be protected for further chemical modification of this scaffold. It is also of note that the triphosphate form of acyclovir is a clinically important antiviral drug, suggesting that other nucleoside prodrugs or their phosphate forms might have off-target activity against SAMHD1. In addition, it is possible that the promiscuous dNTPase activity of SAMHD1 could also degrade the active triphosphate forms of some antiviral and anticancer nucleoside drugs, which has not been thoroughly explored.¹⁹

In summary, we have validated a robust high-throughput assay for screening for inhibitors of SAMHD1. The assay has a large signal-to-background and minimal well-to-well

variability and is appropriate for efficient and economical screening of large compound libraries. In addition, the screen is also applicable for rapid screening of targeted libraries, which has already led to the identification of acyclovir as a potential lead compound for fragment-based drug design. This assay should facilitate the discovery and development of cell-permeable inhibitors of SAMHD1 that will be useful for basic science research in the immunology, virology, and cancer fields and may also lead to new therapeutics.

Supplementary Material

Refer to Web version on PubMed Central for supplementary material.

Acknowledgments

The authors would like to thank Dr. Jun O. Liu and Ruoqing Li for supplying the Hopkins Drug Library and Erik C. Hansen for helpful discussions about this work.

Funding

The authors disclosed receipt of the following financial support for the research, authorship, and/or publication of this article: This work was supported by the National Institutes of Health (NIH) grant T32 GM008763 and NIH grant RO1 GM056834 (J.T.S) and grant 108834-55-RGRL from the Foundation for AIDS Research (J.T.S). K.J.S is the recipient of an American Heart Association Predoctoral Fellowship 14PRE20380664.

References

1. Goldstone DC, Ennis-Adeniran V, Hedden JJ, et al. HIV-1 Restriction Factor SAMHD1 Is a Deoxynucleoside Triphosphate Triphosphohydrolase. *Nature*. 2011; 480:379–382. [PubMed: 22056990]
2. Zhu C, Gao W, Zhao K, et al. Structural Insight into dGTP-Dependent Activation of Tetrameric SAMHD1 Deoxynucleoside Triphosphate Triphosphohydrolase. *Nat Commun*. 2013; 4:2722. [PubMed: 24217394]
3. Ji X, Wu Y, Yan J, et al. Mechanism of Allosteric Activation of SAMHD1 by dGTP. *Nat Struct Mol Biol*. 2013; 20:1304–1309. [PubMed: 24141705]
4. Hansen EC, Seamon KJ, Cravens SL, et al. GTP Activator and dNTP Substrates of HIV-1 Restriction Factor SAMHD1 Generate a Long-Lived Activated State. *Proc Natl Acad Sci US A*. 2014; 111:E1843–E1851.
5. Beloglazova N, Flick R, Tchigvintsev A, et al. Nuclease Activity of the Human SAMHD1 Protein Implicated in the Aicardi-Goutieres Syndrome and HIV-1 Restriction. *J Biol Chem*. 2013; 288:8101–8110. [PubMed: 23364794]
6. Ryou J, Choi J, Oh C, et al. The Ribonuclease Activity of SAMHD1 Is Required for HIV-1 Restriction. *Nat Med*. 2014; 20:936–941. [PubMed: 25038827]
7. Franzolin E, Pontarin G, Rampazzo C, et al. The Deoxynucleotide Triphosphohydrolase SAMHD1 Is a Major Regulator of DNA Precursor Pools in Mammalian Cells. *Proc Natl Acad Sci US A*. 2013; 110:14272–14277.
8. Lahouassa H, Daddacha W, Hofmann H, et al. SAMHD1 Restricts the Replication of Human Immunodeficiency Virus Type 1 by Depleting the Intracellular Pool of Deoxynucleoside Triphosphates. *Nat Immunol*. 2012; 13:223–228. [PubMed: 22327569]
9. Gramberg T, Kahle T, Bloch N, et al. Restriction of Diverse Retroviruses by SAMHD1. *Retrovirology*. 2013; 10:26. [PubMed: 23497255]
10. Hollenbaugh JA, Gee P, Baker J, et al. Host Factor SAMHD1 Restricts DNA Viruses in Non-Dividing Myeloid Cells. *PLoS Pathog*. 2013; 9:e1003481. [PubMed: 23825958]
11. Luban J. Innate Immune Sensing of HIV-1 by Dendritic Cells. *Cell Host Microbe*. 2012; 12:408–418. [PubMed: 23084911]

12. Doitsh G, Galloway NLK, Geng X, et al. Cell Death by Pyroptosis Drives CD4 T-Cell Depletion in HIV-1 Infection. *Nature*. 2014; 505:509–514. [PubMed: 24356306]
13. Rice GI, Bond J, Asipu A, et al. Mutations Involved in Aicardi-Goutières Syndrome Implicate SAMHD1 as Regulator of the Innate Immune Response. *Nat Genet*. 2009; 41:829–832. [PubMed: 19525956]
14. Ramantani G, Häusler M, Niggemann P, et al. Aicardi-Goutières Syndrome and Systemic Lupus Erythematosus (SLE) in a 12-Year-Old Boy with SAMHD1 Mutations. *J Child Neurol*. 2011; 26:1425–1428. [PubMed: 21670392]
15. Crow YJ, Rehwinkel J. Aicardi-Goutières Syndrome and Related Phenotypes: Linking Nucleic Acid Metabolism with Autoimmunity. *Hum Mol Genet*. 2009; 18:R130–R136. [PubMed: 19808788]
16. Clifford R, Louis T, Robbe P, et al. SAMHD1 Is Mutated Recurrently in Chronic Lymphocytic Leukemia and Is Involved in Response to DNA Damage. *Blood*. 2014; 123:1021–1031. [PubMed: 24335234]
17. de Silva S, Wang F, Hake TS, et al. Downregulation of SAMHD1 Expression Correlates with Promoter DNA Methylation in Sézary Syndrome Patients. *J Invest Dermatol*. 2014; 134:562–565. [PubMed: 23884314]
18. Kunz BA. Genetic Effects of Deoxyribonucleotide Pool Imbalances. *Environ Mutagen*. 1982; 4:695–725. [PubMed: 6761109]
19. Huber AD, Michailidis E, Schultz ML, et al. SAMHD1 Has Differential Impact on the Efficacies of HIV Nucleoside Reverse Transcriptase Inhibitors. *Antimicrob Agents Chemother*. 2014; 58:4915–4919. [PubMed: 24867973]
20. Seamon KJ, Hansen EC, Kadina AP, et al. Small Molecule Inhibition of SAMHD1 dNTPase by Tetramer Destabilization. *J Am Chem Soc*. 2014; 136:9822–9825. [PubMed: 24983818]
21. Baykov AA, Evtushenko OA, Avaeva SM. A Malachite Green Procedure for Orthophosphate Determination and Its Use in Alkaline Phosphatase-Based Enzyme Immunoassay. *Anal Biochem*. 1988; 171:266–270. [PubMed: 3044186]
22. Zhang J, Chung T, Oldenburg K. A Simple Statistical Parameter for Use in Evaluation and Validation of High Throughput Screening Assays. *J Biomol Screen*. 1999; 4:67–73. [PubMed: 10838414]
23. Brune M, Hunter JL, Corrie JE, et al. Direct, Real-Time Measurement of Rapid Inorganic Phosphate Release Using a Novel Fluorescent Probe and Its Application to Actomyosin Subfragment 1 ATPase. *Biochemistry*. 1994; 33:8262–8271. [PubMed: 8031761]
24. Arnold LH, Kunzelmann S, Webb MR, et al. A Continuous Enzyme-Coupled Assay for Triphosphohydrolase Activity of HIV-1 Restriction Factor SAMHD1. *Antimicrob Agents Chemother*. 2015; 59:186–192. [PubMed: 25331707]
25. Ugochukwu E, Lovering AL, Mather OC, et al. The Crystal Structure of the Cytosolic Exopolyphosphatase from *Saccharomyces cerevisiae* Reveals the Basis for Substrate Specificity. *J Mol Biol*. 2007; 371:1007–1021. [PubMed: 17599355]
26. Chong CR, Qian DZ, Pan F, et al. Identification of Type 1 Inosine Monophosphate Dehydrogenase as an Antiangiogenic Drug Target. *J Med Chem*. 2006; 49:2677–2680. [PubMed: 16640327]
27. Auda SH, Mrestani Y, Nies DH, et al. Preparation, Physicochemical Characterization and Biological Evaluation of Cefodizime Metal Ion Complexes. *J Pharm Pharmacol*. 2009; 61:753–758. [PubMed: 19505365]
28. Colvin RA, Holmes WR, Fontaine CP, et al. Cytosolic Zinc Buffering and Muffling: Their Role in Intracellular Zinc Homeostasis. *Metallomics*. 2010; 2:306–317. [PubMed: 21069178]
29. Grobler JA, Stillmock K, Hu B, et al. Diketo Acid Inhibitor Mechanism and HIV-1 Integrase: Implications for Metal Binding in the Active Site of Phosphotransferase Enzymes. *Proc Natl Acad Sci US A*. 2002; 99:6661–6666.
30. Jiang YL, Krosky DJ, Seiple L, et al. Uracil-Directed Ligand Tethering: an Efficient Strategy for Uracil DNA Glycosylase (UNG) Inhibitor Development. *J Am Chem Soc*. 2005; 127:17412–17420. [PubMed: 16332091]

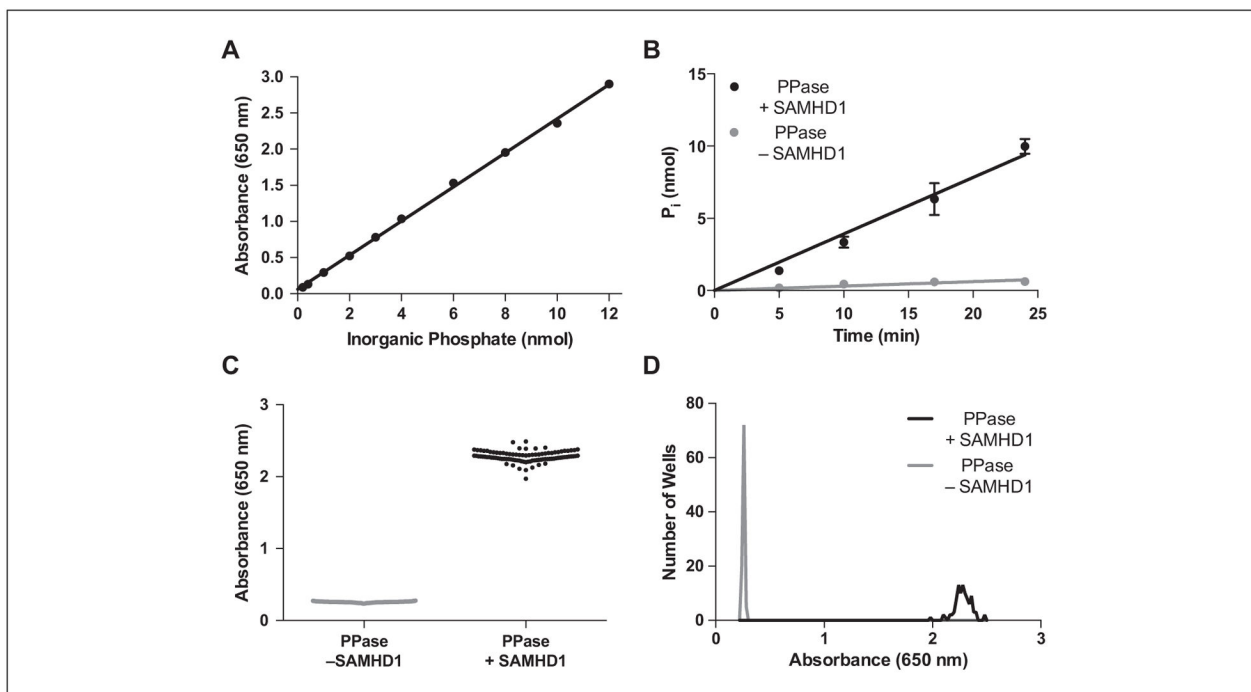


Figure 1.

Development of the enzyme-coupled SAMHD1 assay. **(A)** A standard curve for the detection of inorganic phosphate by malachite green shows a linear response up to 12 nmol of P_i (90 min incubation), which is the maximal amount of phosphate that could be generated in the coupled reaction of SAMHD1 and PPase in the high-throughput screen. **(B)** The rate of phosphate production in the SAMHD1 reaction is linear to 80% dGTP substrate conversion with only trace background activity from PPase. **(C)** Whole-plate replicates of the high-throughput screening reactions in the presence and absence of SAMHD1 showed small well-to-well variability and a large signal change for the SAMHD1 reaction (see Table 1). **(D)** Histogram plots the positive and negative control data in **(C)** showed normal distributions.

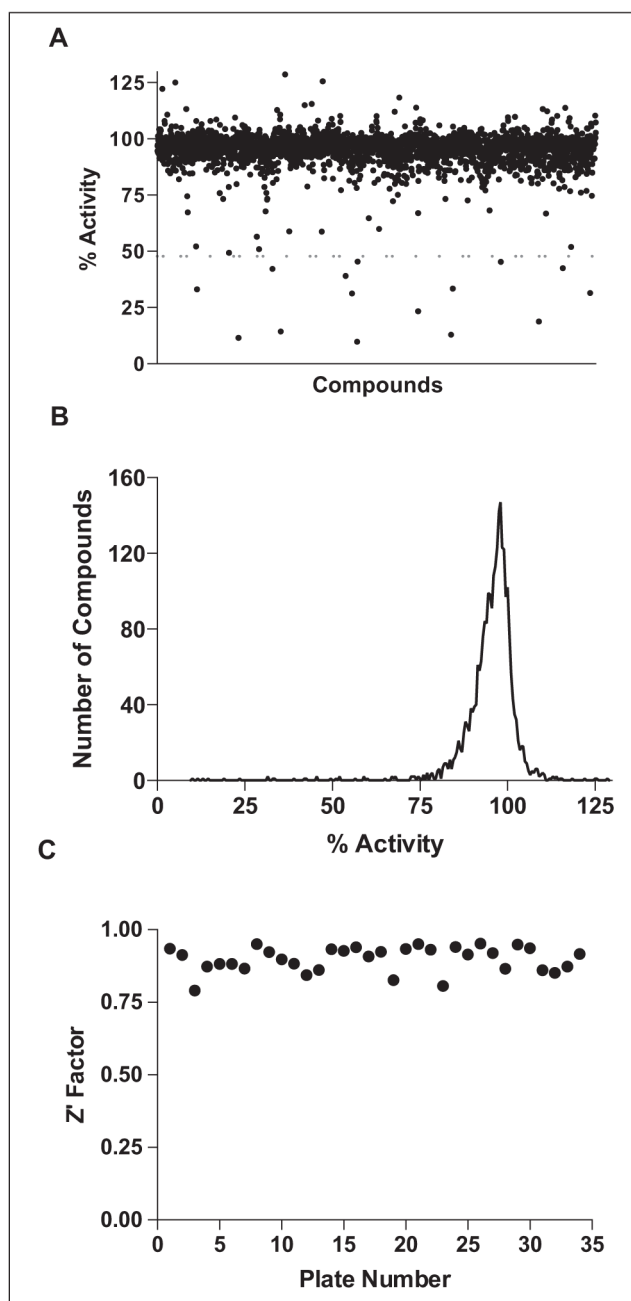
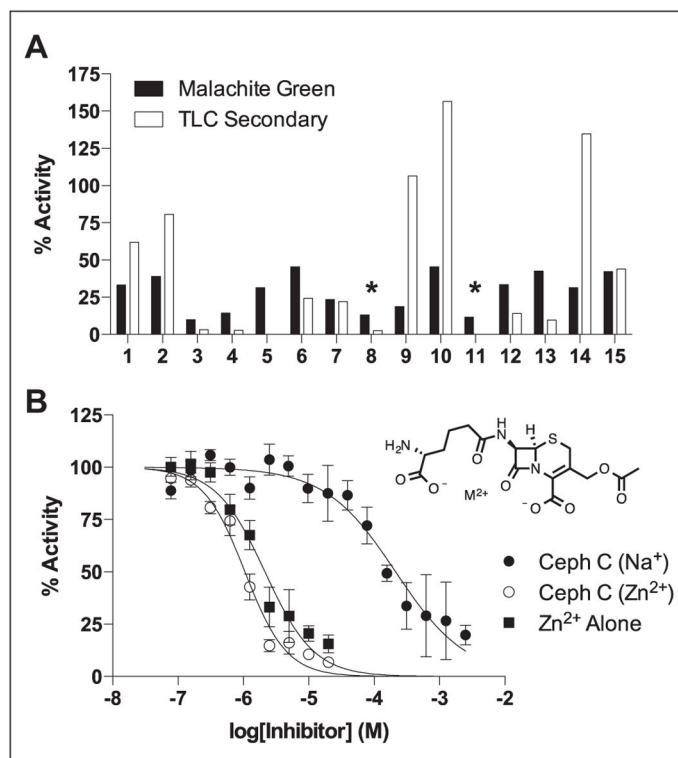


Figure 2. High-throughput screen of the Hopkins library of 2653 clinically used compounds.²⁶ (A) A scatter plot of the SAMHD1 activity (%) in the presence of the library compounds. There were 15 compounds that showed inhibition greater than 6 σ below the mean (dashed line), and these were subjected to secondary screening (0.56%). (B) A histogram plot of the data in (A) shows a slightly tailed distribution as expected if the library contains weak inhibitors. (C) The Z' factors calculated for each of the 34 screening plates ($\langle Z' \rangle = 0.90 \pm 0.04$).

**Figure 3.**

Hit confirmation. **(A)** The 15 hits that showed inhibition greater than 6σ below the mean were tested using a previously described thin-layer chromatography–based activity assay that employs [^3H]dGTP as the substrate. The reaction conditions matched those of the high-throughput screen (HTS). In the secondary screen, only three compounds showed significantly less inhibition than in the direct hydrolysis assay. It is possible that these false-positives could have been inhibitors of the PPase coupling enzyme in the HTS. The asterisks indicate the reactions that contained cephalosporin C. **(B)** Dose-response curves for the two salt forms of cephalosporin C (structure shown). A dose-response curve was also obtained for Zn^{2+} alone (Cl^- counter-ion). See the text for further discussion of the inhibition by these cephalosporins.

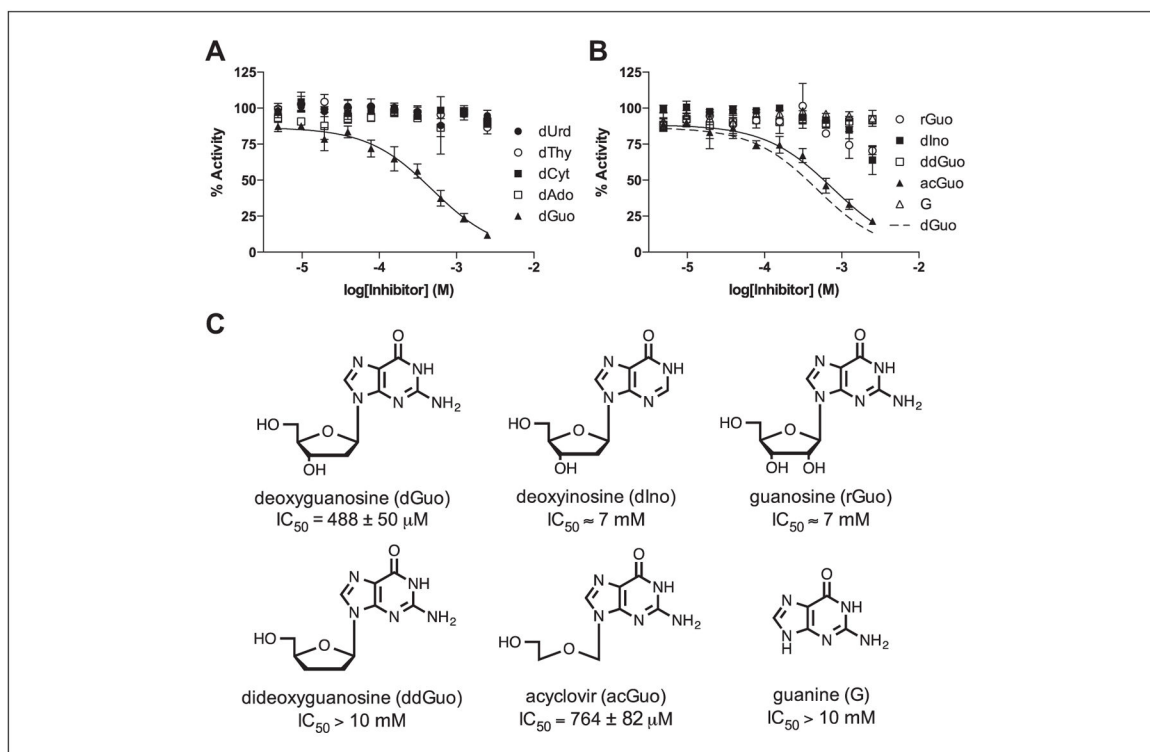


Figure 4. Screening of a targeted library of nucleosides and analogs. **(A)** Dose-response curves were measured for the five canonical deoxyribonucleosides, with only dGuo showing significant inhibition. **(B)** Dose-response curves were measured for a variety of structural analogs of dGuo. Of these, only AcGuo showed similar inhibition to the dGuo. **(C)** Structures and calculated IC₅₀ values for dGuo and the other guanine analogs.

Table 1Optimized 96-Well High-Throughput Screening Parameters and Assay Statistics.^a

SAMHD1	0.5 μ M
PPase	5 μ M
dGTP (activator/substrate)	0.1 mM ($\sim 1/10 K_m^{dGTP}$) ^b
Total reaction volume and time	40 μ L and 20 min
Z' factor	0.87
Mean signal (\pm SD)	
Positive control ^c	2.28 \pm 0.08
Negative control ^d	0.26 \pm 0.01
Coefficient of variation of signal, %	
Positive control	3.4
Negative control	3.3
Signal/background ^e	9

^aThe volumes would be reduced by 50% for a 384-well plate format.

^bSee reference 4 for the steady-state kinetic parameters of SAMHD1.

^cThe mean measured absorbance for 96 reactions carried out using the indicated conditions.

^dThe mean measured absorbance for 96 reactions carried out in the absence of SAMHD1.

^eCalculated from the ratio of the mean signals for the positive and negative controls.